



Comparative Study of Novel *N*-Substituted Quinoxaline Derivatives towards Mild Steel Corrosion in Hydrochloric Acid: Part 1

F. El-Hajjaji¹, B. Zerga¹, M. Sfaira^{1,*}, M. Taleb¹, M. Ebn Touhami², B. Hammouti³,
S.S. Al-Deyab⁴, H. Benzeid⁵, El M. Essassi⁵

¹ Laboratoire d'Ingénierie des Matériaux, de Modélisation et d'Environnement, LIMME, Faculté des Sciences Dhar El Mahraz, Université Sidi Mohammed Ben Abdellah, USMBA, BP 1796 – 30000, Atlas – Fès, Morocco.

² LM2E, Faculté des Sciences, Université Ibn Tofaïl, BP. 133 – 14000, Kénitra, Morocco.

³ LCAE-URAC18, Faculté des Sciences, Université Mohammed Premier, BP 717 – 60000, Oujda, Morocco.

⁴ Department of Chemistry, College of Science, King Saud University, B.O. 2455, Riaydh11451, Saudi Arabia.

⁵ Laboratoire de Chimie Organique Hétérocyclique, Pôle de Compétences Pharmacochimie, Faculté des Sciences, Université Mohammed V Rabat – Morocco.

Received 12 April 2013, Revised 25 July 2013, Accepted 25 July 2013

*E-mail: msfaira@yahoo.com

Abstract

The inhibitive effect of four quinoxaline derivatives named 1-ethyl-3-methylquinoxalin-2(1H)-one (Et-N-Q=O), 1-benzyl-3-methylquinoxalin-2(1H)-one (Bz-N-Q=O), 3-methyl-1-prop-2-ynylquinoxalin-2(1H)-one (Pr-N-Q=O) and 3-methyl-1-prop-2-ynylquinoxaline-2(1H)-thione (Pr-N-Q=S), on the corrosion of mild steel in hydrochloric acid 1 M has been investigated at 308 K. The study was carried out using weight loss measurements, potentiodynamic polarisation and electrochemical impedance spectroscopy (EIS) methods. The obtained results showed that Pr-N-Q=S and Pr-N-Q=O were the best inhibitors and their inhibition efficiencies increased with the increase of inhibitor concentration and reached up to 92 % for Pr-N-Q=O and 93 % for Pr-N-Q=S at 10⁻³ M. Potentiodynamic polarisation studies clearly revealed that the presence of these inhibitors did not change the mechanism of hydrogen evolution and that they acted as mixed-type inhibitors with predominance at cathodic range. EIS measurements showed that the charge transfer resistance increases whereas the double layer capacitance decreases with the inhibitor concentration. The effect of temperature is studied and determination of the activation and adsorption parameters is discussed separately in part 2 and part 3 for Pr-N-Q=O and Pr-N-Q=S, respectively. In part 4, quantum chemical calculations were undertaken to correlate the structure electronic properties with corrosion inhibition efficiency for all studied quinoxaline molecules.

Keywords: Quinoxaline derivatives; Corrosion inhibition; Mild steel; Hydrochloric acid; Adsorption.

1. Introduction

Mild steel is widely employed in industry because of its low cost and availability. As a result of its industrial concern, attention has been paid to study and to prevent this metal against corrosion in different media [1-26]. Acid solutions are generally used for the removal of undesirable scale and rust in several industrial processes. The most important areas of application are acid pickling, oil well acidizing, acid cleaning and acid descaling, etc. Because of the general aggressiveness of acids, inhibitors are often used to control attack of acid environment and to reduce the overall corrosion current density. The inhibition of corrosion in acid solutions can be secured by the addition of a variety of organic compounds and has been widely investigated in our laboratory [7-26]. Most of the well-known acid inhibitors are organic compounds containing P, S, O and/or N atoms. However, the use of organic inhibitors in acid solutions can, in some cases, lead to enhancement of the metal corrosion [27], and stimulation of corrosion is related not only to the type and structure of the organic molecule but also depends on the type of acid and its concentration [28]. The mechanism of organic corrosion inhibitors is usually linked to adsorption phenomenon because of the presence of heteroatoms, aromatic rings... called active centres of adsorption. Two possible modes of adsorption are well-known: physical adsorption and/or chemical adsorption. The corrosion inhibition, normally considered by corrosion scientists, is the relation between the molecular/electronic structures and corrosion inhibition efficiency. Quinoxaline and its derivatives are, among

compounds, which present corrosion inhibition performance of iron and aluminium in HCl aqueous solution as reported in references [22, 26, 29-32].

The objective of this study is to test four quinoxaline derivatives newly synthesized as corrosion inhibitors of mild steel in 1 M HCl. Measurements were carried out with potentiodynamic polarization and electrochemical impedance spectroscopy measurements and gravimetric method.

2. Experimental details

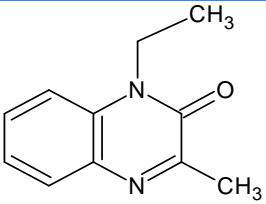
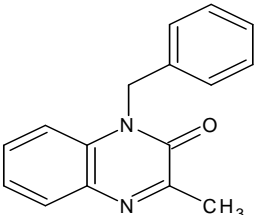
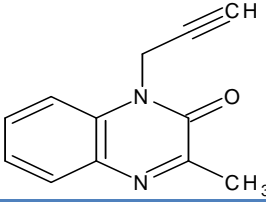
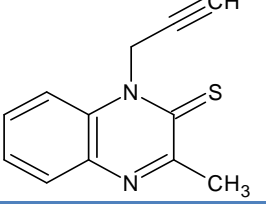
2.1. Materials and reagents

Mild steel strips containing (in wt%) 0.09 P, 0.38 Si, 0.01 Al, 0.05 Mn, 0.21 C, 0.05 S and balance iron were used for electrochemical and gravimetric studies. Mild steel specimens were mechanically polished on wet SiC papers (400, 600, 1000 and 1200), washed with double-distilled water, and dried at room temperature before being immersed in the acid solution. The aggressive solution (1 M HCl), used as blank, was made from Riedel-de Haën and prepared by dilution of analytical grade 37%. The molecular structures of the studied quinoxaline, names and the corresponding abbreviations are shown in Table 1. Appropriate concentrations of inhibitors were prepared with double-distilled water addition. The concentration range of inhibitors employed was 10^{-6} – 10^{-3} M in 1 M HCl. The temperature was controlled at 308 K without bubbling in a double walled glass cell.

2.2. Electrochemical measurements

For electrochemical measurements, a conventional three-electrode glass cell with a platinum counter electrode (CE) and a saturated calomel electrode (SCE) as reference (RE) was used. All potentials were measured against SCE. Mild steel cylindrical rod of the same composition as working electrode (WE) was pressure fitted into a polytetrafluoroethylene holder (PTFE) to avoid any infiltration of electrolyte then exposing only 1 cm² surface to the aggressive solution. The test solution was thermostatically controlled at 35 °C in air atmosphere without bubbling.

Table 1. Molecular structures, names and abbreviations of the undertaken quinoxaline molecules

Quinoxaline Formula	Name	Abbreviation
	1-ethyl-3-methylquinoxalin-2(1H)-one	Et-N-Q=O
	1-benzyl-3-methylquinoxalin-2(1H)-one	Bz-N-Q=O
	3-methyl-1-prop-2-ynylquinoxalin-2(1H)-one	Pr-N-Q=O
	3-methyl-1-prop-2-ynylquinoxaline-2(1H)-thione	Pr-N-Q=S

The polarization curves were recorded by changing the electrode potential automatically with a Potentiostat/Galvanostat type PGZ 100, at a scan rate of 1 mV s⁻¹ and controlled with analysis software (Voltmaster 4). Before each experiment, the working electrode was immersed in the test cell for an hour until reaching steady state.

The data in Tafel region have been processed for evaluation of corrosion kinetic parameters by plotting the polarization curves. The linear Tafel segments, in a large domain of potential, of the cathodic curves were extrapolated to the corresponding corrosion potentials to obtain the corrosion current values. The inhibition efficiency was evaluated using the relationship 1:

$$IE_{i-E} = \frac{i_{corr}^0 - i_{corr}}{i_{corr}^0} \times 100 \quad (1)$$

where i_{corr}^0 and i_{corr} are the corrosion current densities values without and with inhibitors, respectively.

The electrochemical impedance spectroscopy measurements were carried out using a transfer function analyser (Radiometer-analytical PGZ 100), with a small amplitude ac. signal (10 mV rms), over a frequency domain from 100 KHz to 10 mHz at 303 K and in air atmosphere. To determine the impedance parameters of the mild steel specimens in acidic solution, the measured impedance data were analyzed using Bouckamp program based upon an electric equivalent circuit [33]. The charge transfer resistance R_{ct} , is obtained from the diameter of the semicircle in the Nyquist representation. The inhibition efficiency of the inhibitors got from EIS measurements has been determined from the relationship 2:

$$IE_{imp} \% = \frac{R_{ct} - R_{ct}^0}{R_{ct}} \times 100 \quad (2)$$

where R_{ct}^0 and R_{ct} are the charge transfer resistance values in the absence and in the presence of inhibitor, respectively.

2.3. Weight loss measurements

Gravimetric experiments were carried out in a double walled glass cell equipped with a thermostat cooling condenser. The solution volume was 100 cm³ and the temperature of 308 K was controlled thermostatically. The mild steel specimens were squarer in the form (2cm×2cm×0.05cm). The weight loss of mild steel in 1 M HCl with and without addition of inhibitors was determined after an immersion period in acid of 6 h. After the corrosion test, the specimens were carefully washed in double distilled water, dried and then weighted. Duplicate experiments were performed in each case, and the mean value of the weight loss is reported. Weight loss allowed us to calculate the mean corrosion rate as expressed in mg cm⁻² h⁻¹. The resulting quantity, corrosion rate, W_{corr} , is thereby the fundamental measurement in corrosion. W_{corr} can be determined either by chemical analysis of dissolved metal in solution or by gravimetric method measuring weight of specimen before and after exposure in the aggressive solution applying the following equation 3:

$$W_{corr} = \frac{m_i - m_f}{S t} \quad (3)$$

where m_i , m_f , S and t denote initial weight, final weight, surface of specimen and immersion time, respectively. The inhibition efficiency $E_{WL}\%$ derived from this method was estimated by the following relation 4:

$$IE_{WL} \% = \frac{W_{corr} - W_{corr/inh}}{W_{corr}} \times 100 \quad (4)$$

where W_{corr} and $W_{corr/inh}$ are the corrosion rate of steel without and with each inhibitor, respectively.

3. Results and discussion

3.1. Polarisation curves

Figure 1 presents the potentiodynamic polarization curves of mild steel in 1 M HCl without and with the studied inhibitors at 10⁻³ M and 303 K. As it can be seen, only cathodic reaction is affected by the presence of Et-N-Q=O and Bz-N-Q=O, whereas both cathodic and anodic reactions of mild steel electrode corrosion are inhibited in the presence of Pr-N-Q=O and Pr-N-Q=S. The corrosion potential remains, for all inhibitors, circa constant. These finding stipulate that Et-N-Q=O and Bz-N-Q=O act as cathodic-type inhibitors while Pr-N-Q=O and Pr-N-Q=S perform as mixed-type inhibitors.

Figures 2 and 3 show more details in terms of concentration effect of Pr-N-Q=O and Pr-N-Q=S. Pr-N-Q=O appears to slow down the cathodic reaction to greater extents than the anodic one especially at low concentrations whereas at 10⁻⁴ M and more the anodic branch is affected and Pr-N-Q=O depends upon electrode potential. It is also observed that for potentials higher than -200 mVsce, the Pr-N-Q=O starts to be desorbed. In this case desorption of Pr-N-Q=O is raised more than its adsorption. However, in the presence of Pr-N-Q=S and at all

studied concentrations, among the decrease of cathodic branch, the anodic one shows similar behaviour without being dependant on potential. These results suggest that the addition of quinoxaline derivatives under study reduce anodic dissolution of mild steel for Pr-N-Q=S and also retard the hydrogen evolution reaction for the studied inhibitors. Cathodic current potential curves give rise to parallel Tafel lines indicating that the hydrogen discharge is activation-controlled and the addition of quinoxaline derivatives does not affect the mechanism process of hydrogen reduction.

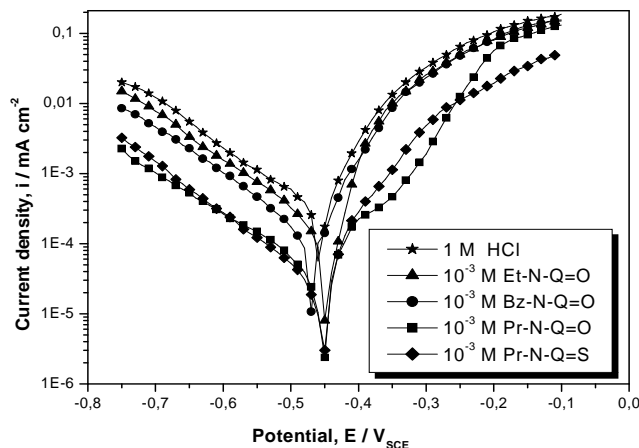


Figure 1. Polarisation curves for Mild steel in 1 M HCl at 10^{-3} M of all the quinoxaline molecules

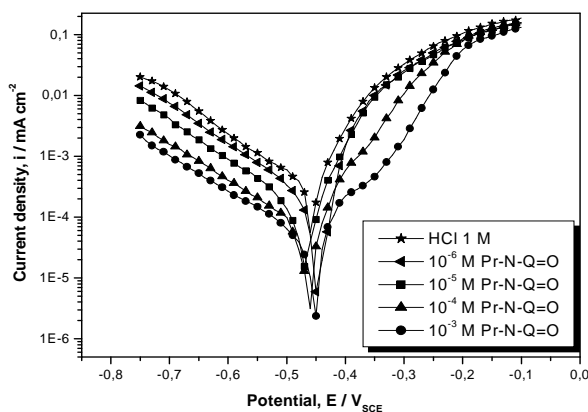


Figure 2. Potentiodynamic polarization curves obtained for mild steel in 1 M HCl at various concentrations of Pr-N-Q=O.

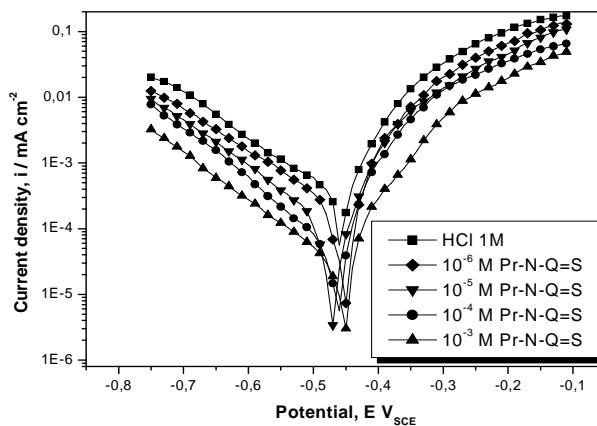


Figure 3. Potentiodynamic polarization curves obtained for mild steel in 1 M HCl at various concentrations of Pr-N-Q=S

The electrochemical parameters (i_{corr} , E_{corr} , b_c and $IE_{i-E}\%$) derived from i - E characteristics for the four studied inhibitors are given in Table 2. The results drawn on Table 2 clearly exemplify a decrease in the corrosion rate in the presence of all products. This effect is hugely marked at higher concentration of quinoxaline inhibitors. For the inhibitors, Et-N-Q=O and Bz-N-Q=O especially studied at 10^{-3} M gave only 44 and 48 %, respectively as $IE_{i-E}\%$ at the limit of their solubility. The authors have suggested uninteresting to expand more studies neither at lower concentrations nor with other techniques. Cathodic Tafel slopes (b_c), are approximately constant, meaning that the inhibiting action of these molecules occurred by simple blocking of the available surface area; i.e. the inhibitors decreased the surface area for hydrogen evolution without affecting the reaction mechanism [34]. The decrease of i_{corr} indicates that the addition of quinoxaline inhibits the corrosion process by decreasing the surface area for corrosion. The efficiency obtained shows that the inhibitory effect of quinoxaline tested increases in the following sequence: Pr-N-Q=S > Pr-N-Q=O > Bz-N-Q=O > Et-N-Q=O.

Table 2. Polarization parameters and corresponding inhibition efficiency for the mild steel corrosion in 1 M HCl without and with addition of various concentrations of quinoxaline molecules

Inhibitor	Concentration C / M	E_{corr} mV _{sce}	$-b_c$ mV dec ⁻¹	i_{corr} $\mu A cm^{-2}$	IE_{i-E} %
Blank	00	-460	160	350	—
Et-N-Q=O	1×10^{-3}	-450	165	196	44.0
Bz-N-Q=O	1×10^{-3}	-470	169	182	48.0
Pr-N-Q=O	1×10^{-6}	-460	160	200	42.8
	1×10^{-5}	-460	180	140	60.0
	1×10^{-4}	-470	180	57	83.7
	1×10^{-3}	-450	170	35	90.0
Pr-N-Q=S	1×10^{-6}	-450	140	176	49.7
	1×10^{-5}	-470	130	110	68.6
	1×10^{-4}	-460	150	50	85.7
	1×10^{-3}	-450	160	23	93.4

3.2. Electrochemical impedance spectroscopy measurements

Figures 4 and 5 present the Nyquist diagrams obtained in the absence and presence of Pr-N-Q=O and Pr-N-Q=S at different concentrations. A depressed semicircle, as often obtained in acidic media [10,11] can be seen. The difference from theoretical results is generally attributed to Cole-Cole [3,35] and/or Cole-Davidson [36] representations inherent to frequency dispersion. This phenomenon is generally attributed to different physical processes such as the non-homogeneity of the electrode surface or its roughness during the corrosion process [37], adsorption of inhibitors [38], and formation of porous layers [39]. The existence of single semicircle relates the presence of single charge-transfer process, which is unaffected by the presence of Pr-N-Q=O and Pr-N-Q=S. According to a classical method, the EIS spectra of Figs. 4 and 5 will be interpreted in terms of parallel R_{ct} - C_{dl} circuit.

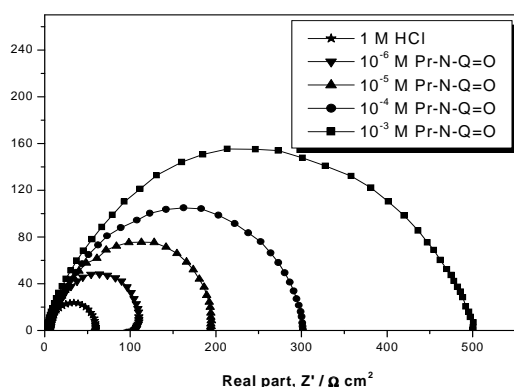


Figure 4. Nyquist diagrams of mild steel in 1M HCl without and with different concentrations of Pr-N-Q=O

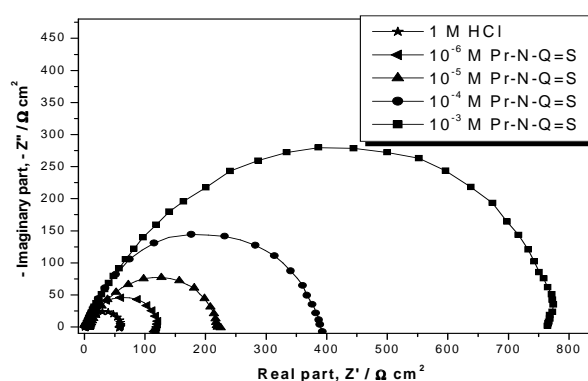


Figure 5. Nyquist diagrams of mild steel in 1M HCl without and with different concentrations of Pr-N-Q=S

It is clear from these spectra that the impedance response of mild steel in the absence of inhibitors has significantly changed, in size, after the addition of Pr-N-Q=O and Pr-N-Q=S into the corrosive medium. Indeed that the impedance of inhibited electrode increases with increasing inhibitors concentration and consequently the inhibition efficiency increases as it is explained hereafter.

The impedance parameters calculated are given in Table 3. The charge-transfer resistance values (R_{ct}) are calculated from the difference in impedance at lower and higher frequencies. The double layer capacitances (C_{dl}) are obtained at the frequency at which the imaginary component of the impedance is maximum ($-Z''_{max}$) as follows in equation 5:

$$f(-Z''_{i_{max}}) = \frac{1}{2\pi C_{dl} R_{ct}} \quad (5)$$

Table 3. EIS parameters for the Mild steel corrosion in 1 M HCl at different concentrations of Pr-N-Q=O and Pr-N-Q=S.

Inhibitor	Concentration C / M	R_{ct} Ω cm ²	C_{dl} μ F cm ⁻²	IE _{imp} %
HCl	00	60	490	—
Pr-N-Q=O	1 x 10 ⁻⁶	110	82	45.5
	1 x 10 ⁻⁵	195	71	69.2
	1 x 10 ⁻⁴	300	45	80.0
	1 x 10 ⁻³	500	36	88.8
Pr-N-Q=S	1 x 10 ⁻⁶	120	175	50.0
	1 x 10 ⁻⁵	220	70	72.7
	1 x 10 ⁻⁴	390	20	84.6
	1 x 10 ⁻³	775	13	92.3

From the impedance parameters, one can conclude that the values of R_{ct} increase with rise concentration of Pr-N-Q=O and Pr-N-Q=S then accordingly points out an increase in the corrosion inhibition efficiency. This evolution indicates that the charge-transfer process mainly control the corrosion of mild steel. The values of double layer capacitance are brought down to the maximum extend in the presence of Pr-N-Q=O and Pr-N-Q=S and the decrease of C_{dl} follows the order similar to that obtained for i_{corr} obtained from i - E characteristics. If one assumes that the double layer between the charged surface and the electrolyte is considered as an electrical capacitor, the adsorption of Pr-N-Q=O and Pr-N-Q=S on the electrode may decrease the electrical capacity because the inhibitor displaces the water molecules or even others ions originally adsorbed on the electrode. Thus the decrease of C_{dl} with rise in concentration of Pr-N-Q=O and Pr-N-Q=S is in favour of selectively adsorption of Pr-N-Q=O and Pr-N-Q=S in specific places [40] and/or formation of complex onto the metal surface [41]. According to this inhibition mechanism Pr-N-Q=O and Pr-N-Q=S maybe adsorbed at active points causing the corrosion rate to drop.

The values of inhibition efficiency obtained from EIS measurements for the tested inhibitors follow the order Pr-N-Q=S > Pr-N-Q=O. The EIS results correspond to those obtained from polarization tests.

3.3 Gravimetric measurements

The effect of addition of Et-N-Q=O, Bz-N-Q=O, Pr-N-Q=O and Pr-N-Q=S at different concentrations on the corrosion of mild steel in 1 M HCl solution is also studied by weight loss at a temperature of 308 K. Table 4 gathers the deduced values of W_{corr} and $IE_{WL}\%$.

Gravimetric measurements show that the corrosion decreases in the presence of Pr-N-Q=S, Pr-N-Q=O, Bz-N-Q=O and Et-N-Q=O. The inhibitive action is better expressed by the inhibition efficiency which increases with inhibitor concentration to reach 95.6 and 92.2% at 10⁻³ M for Pr-N-Q=S and Pr-N-Q=O, respectively. Thus all inhibitors studied inhibit the corrosion of mild steel in 1 M HCl, but Pr-N-Q=S is found to be the best one.

It the case of Pr-N-Q=O and Pr-N-Q=S, it is shown that the weight-loss decreases whereas the inhibition efficiency increases with rise of concentration of these compounds. The corrosion inhibition can be imputed to the adsorption of quinoxaline derivatives at the steel/acid solution interface like various sulphur and oxygen compounds studied as effective corrosion inhibitors in acidic media. Maximum of $IE_{WL}\%$ is achieved at 10⁻³ M. Thus at 35 °C, the quinoxaline molecules line according to their inhibiting efficiency is as follows: Pr-N-Q=S > Pr-N-Q=O > Bz-N-Q=O > Et-N-Q=O

The high inhibitive performance of Pr-N-Q=S and Pr-N-Q=O suggests a strong bonding of this quinoxaline molecules onto the metal surface due to the presence of several lone pairs from heteroatom (oxygen and sulphur) and π -orbitals, blocking the active sites and therefore decreasing the corrosion rate. Moreover, the high $IE_{WL}\%$ of Pr-N-Q=S than Pr-N-Q=O can be imputed to the presence of thioxo group on the quinoxaline ring, which gives the

possibility of $d\pi-d\pi$ bond formation resulting from overlap of 3d electrons from Fe atom and the 3d vacant orbital of sulphur atom [19,22,26]. More explanations will be given in part 4 under progress concerning the quantum chemical calculation of global and local descriptors at B3LYP/6.31G(d,p) level of theory.

Table 4. Corrosion rate of mild steel and inhibition efficiency at different concentrations of Quinoxaline derivatives in 1 M HCl obtained from weight loss measurements at 308 K after 6 h of immersion

Inhibitor	Concentration C / M	Weight loss $W_{\text{corr}} / \text{mg cm}^{-2} \text{ h}^{-1}$	IE _{WL} %
Blank	00	1.15	–
Et-N-Q=O	1×10^{-3}	0.625	45.6
Bz-N-Q=O	1×10^{-3}	0.515	55.2
Pr-N-Q=O	1×10^{-6}	0.68	40.9
	1×10^{-5}	0.52	54.8
	5×10^{-5}	0.33	71.3
	1×10^{-4}	0.19	83.5
	5×10^{-4}	0.11	90.4
	1×10^{-3}	0.09	92.2
	Pr-N-Q=S	1×10^{-6}	0.62
1×10^{-5}		0.45	60.8
5×10^{-5}		0.29	74.8
1×10^{-4}		0.15	86.9
5×10^{-4}		0.08	93.0
1×10^{-3}		0.05	95.6

Conclusion

On the basis of these results, it can be drawn:

- * Pr-N-Q=O and Pr-N-Q=S present best performances as corrosion inhibitors for mild steel in 1 M HCl when compared to Et-N-Q=O and Bz-N-Q=O.
- * Potentiodynamic polarisation studies reveal that the presence of inhibitors does not change the mechanism of hydrogen evolution.
- * Pr-N-Q=O and Pr-N-Q=S act as mixed inhibitors with predominance at cathodic range.
- * Impedance method indicates that quinoxaline compounds adsorb on mild steel surface with increasing charge transfer resistance and decreasing the double-layer capacitance.
- * The weight loss method shows that the inhibition efficiency increases with increasing of inhibitor concentration to attain a maximum value of 92.2 and 95.6 % for Pr-N-Q=O and Pr-N-Q=S, respectively at 10^{-3} M.
- * Results derived for the undertaken methods are in good agreement.

References

1. Sfaira M., Srhiri A., Keddami M., Takenouti H., *Electrochim. Acta*, 44 (1999) 4395.
2. Sfaira M., Srhiri A., Takenouti H., De Ficquelmont-Loizos M.M., Ben Bachir A., Khalakhil M., *J. Appl. Electrochem.*, 31 (2001) 537.
3. Duval S., Keddami M., Sfaira M., Srhiri A., Takenouti H., *Electrochem. Soc. Proc.* 22 (2001) 557.
4. Duval S., Keddami M., Sfaira M., Srhiri A., Takenouti H., *J. Electrochem. Soc.* 149 (2002) B520.
5. Tourir R., Dkhireche N., Ebn Touhami M., Lakhri M., Lakhri B., Sfaira M., *Desalination*, 249 (2009) 922.
6. Tourir R., Dkhireche N., Ebn Touhami M., Sfaira M., Senhaji O., Robin J.J., Boutevin B., Cherkaoui M., *Mater. Chem. Phys.*, 122 (2010) 1.
7. Labriti B., Dkhireche N., Tourir R., Ebn Touhami M., Sfaira M., El Hallaoui A., Hammouti B., Alami A., *Arab. J. Sci. Eng.*, (2012) DOI 10.1007/s13369-012-0257-7.
8. Dkhireche N., Abdelhadi R., Ebn Touhami M., Oudda H., Tourir R., Sfaira M., Hammouti B., Senhaji O., Taouil R., *Int. J. Electrochem. Sci.*, 7 (2012) 5314.
9. Zerga B., Sfaira M., Rais Z., Ebn Touhami M., Taleb M., Hammouti B., Imelouane B., Elbachiri A., *Matér. & Tech.*, 97 (2009) 297.
10. Aloui S., Forsal I., Sfaira M., Ebn Touhami M., Taleb M., Filali Baba M., Daoudi M., *Port. Electrochim. Acta*, 27 (2009) 599.
11. Zerga B., Attayibat A., Sfaira M., Taleb M., Hammouti B., Ebn Touhami M., Radi S., Rais Z., *J. Appl. Electrochem.*, 40 (2010) 1575.

12. Adardour K., Kassou O., Tourir R., Ebn Touhami M., ElKafsaoui H., Benzeid H., Essassi El M., Sfaira M., *J. Mater. Environ. Sci.*, 1 (2010) 129.
13. Cisse M.B., Zerga B., Kalai F. El., Ebn Touhami M., Sfaira M., Taleb M., Hammouti B., Benchat N., El Kadiri S., Benjelloun A.T., *Surf. Rev. Lett.*, 18 (2011) 303.
14. Zerga B., Sfaira M., Taleb M., Ebn Touhami M., Hammouti B., Attayibat A., Radi S., Benjelloun A.T., *Der Phar. Chem.*, 4 (2012) 1887.
15. El Khattabi O., Zerga B., Sfaira M., Taleb M., Ebn Touhami M., Hammouti B., Herrag L., Mcharfi M., *Der. Phar. Chem.*, 4 (2012) 1759.
16. Aderdour K., Tourir R., Ebn Touhami M., Sfaira M., El Kafssaoui H., Hammouti B., Benzaid H., Essassi El M., *Der Phar. Chem.*, 4 (2012) 1485.
17. Zerga B., Saddik R., Hammouti B., Taleb M., Sfaira M., Ebn Touhami M., Al-Deyab S.S., Benchat N., *Int. J. Electrochem. Sci.*, 7 (2012) 631.
18. B. Zerga, B. Hammouti, M. Ebn Touhami, R. Tourir, M. Taleb, M. Sfaira, M. Bennajeh, I. Forssal, *Int. J. Electrochem. Sci.*, 7 (2012) 471.
19. El Adnani Z., Mcharfi M., Sfaira M., Benjelloun A.T., Benzakour M., Ebn Touhami M., Hammouti B., Taleb M., *Int. J. Electrochem. Sci.*, 7 (2012) 3982.
20. Aouine Y., Sfaira M., Ebn Touhami M., Alami A., Hammouti B., Elbakri M., El Hallaoui A., Tourir R., *Int. J. Electrochem. Sci.*, 7 (2012) 5400.
21. Benbouya K., Zerga B., Sfaira M., Taleb M., Ebn Touhami M., Hammouti B., Benzeid H., Essassi E.M., *Int. J. Electrochem. Sci.*, 7 (2012) 6313.
22. El Adnani Z., Mcharfi M., Sfaira M., Benzakour M., Benjelloun A.T., Ebn Touhami M., Hammouti B., Taleb M., *Int. J. Electrochem. Sci.*, 7 (2012) 6738.
23. Niouri W., Zerga B., Sfaira M., Taleb M., Hammouti B., Ebn Touhami M., Al-Deyab S.S., Benzeid H., Essassi El M., *Int. J. Electrochem. Sci.*, 7 (2012) 10190.
24. Elbakri M., Tourir R., Ebn Touhami M., Zarrouk A., Aouine Y., Sfaira M., Bouachrine M., Alami A., El Hallaoui A., *Res. Chem. Intermed.* (2012) DOI 10.1007/s11164-012-0768-6.
25. Elkacimi Y., Achnin M., Aouine Y., Ebn Touhami M., Alami A., Tourir R., Sfaira M., Chebabe D., Elachqar A., Hammouti B., *Portug. Electrochim. Acta*, 30 (2012) 53.
26. El Adnani Z., Mcharfi M., Sfaira M., Benzakour M., Benjelloun A.T., Ebn Touhami M., *Corros. Sci.*, 68 (2013) 223.
27. Lagrenée M., Mernari B., Chaibi N., Traisnel M., Vezin H., Bentiss F., *Corros. Sci.*, 43 (2001) 951.
28. Elayyachy M., Hammouti B., El Idrissi A., Aouniti A., *Portug. Electrochim. Acta*, 29 (2011) 57.
29. Zarrouk A., Dafali A., Hammouti B., Zarrok H., Boukhris S., Zertoubi M., *Int. J. Electrochem. Sci.* 5 (2010) 46.
30. El Ouali I., Hammouti B., Aouniti A., Ramli Y., Azougagh M., Essassi El M., Bouachrine M., *J. Mater. Environ. Sci.*, 1 (2010) 1.
31. Elayyachy M., Hammouti B., El Idrissi A., Aouniti A., *Portug. Electrochim. Acta.*, 29 (2011) 57.
32. Hammouti B., Zarrouk A., Al-Deyab S.S., *Oriental J. Chem.*, 27 (2011) 23.
33. Bouckamp A., *Users Manual Equivalent Circuit, ver. 4.* 51 (1993).
34. Abdel Aal M.S., Radwan S., El Saied A., *Br. Corros. J.* 18 (1983) 2.
35. Cole K.S., Cole R.H., *J. Chem. Phys.* 9 (1941) 341.
36. Davidson D.W., Cole R.H., *J. Chem. Phys.* 19 (1951) 1484.
37. Juttner K., *Electrochim. Acta* 35 (1990) 1501.
38. Bentiss F., Traisnel M., Gengembre L., Lagrenée M., *Appl. Surf. Sci.*, 152 (1999) 237.
39. Bentiss F., Traisnel M., Lagrenée M., *Br. Corros. J.*, 35 (2000) 315.
40. Bastidas J.M., Polo J.L., Cano E., Torres C.L., *J. Mater. Sci.*, 35 (2000) 2637.
41. Chetouani A., Daoudi M., Hammouti B., Ben Hadda T., Benkaddour M., *Corros. Sci.*, 48, (2006) 2987.

(2014) ; <http://www.jmaterenvirosnci.com>